Optical Multi-Gas Monitor Technology Demonstration on the International Space Station

Jeffrey S. Pilgrim[1], William R. Wood [2], Miguel. E. Casias[3] and Andrei B. Vakhtin[4]
Vista Photonics, Inc., Santa Fe, New Mexico 87508-9463

Michael D. Johnson[5]
NanoRacks LLC, Houston, Texas, 77058

and

Paul D. Mudgett[6]
NASA Johnson Space Center, Houston, Texas, 77058

The International Space Station (ISS) employs a suite of portable and permanently located gas monitors to insure crew health and safety. These sensors are tasked with functions ranging from fixed mass spectrometer based major constituents analysis to portable electrochemical sensor based combustion product monitoring. An all optical multi-gas sensor is being developed that can provide the specificity of a mass spectrometer with the portability of an electrochemical cell. The technology, developed under the Small Business Innovation Research program, allows for an architecture that is rugged, compact and low power. A four gas version called the Multi-Gas Monitor was launched to ISS in November 2013 aboard Soyuz and activated in February 2014. The portable instrument is comprised of a major constituents analyzer (water vapor, carbon dioxide, oxygen) and high dynamic range real-time ammonia sensor. All species are sensed inside the same enhanced path length optical cell with a separate vertical cavity surface emitting laser (VCSEL) targeted at each species. The prototype is controlled digitally with a field-programmable gate array/microcontroller architecture. The optical and electronic approaches are designed for scalability and future versions could add three important acid gases and carbon monoxide combustion product gases to the four species already sensed. Results obtained to date from the technology demonstration on ISS are presented and discussed.

[1]President, 3 N. Chamisa Drive, Suite 1, Santa Fe, New Mexico 87508-9463, Senior Member.
[2]Senior Research Engineer, 3 N. Chamisa Drive, Suite 1, Santa Fe, New Mexico 87508-9463, Member.
[3]Senior Research Engineer, 3 N. Chamisa Drive, Suite 1, Santa Fe, New Mexico 87508-9463.
[4]Principal Research Scientist, 3 N. Chamisa Drive, Suite 1, Santa Fe, New Mexico 87508-9463.
[5]Chief Technology Officer, 18100 Upper Bay Road, Suite 150, Houston, TX 77058.
[6]Laboratory Technical Monitor, 2101 NASA Parkway, Houston, TX 77058, Mail Code SK4.

Nomenclature

AC	=	alternating current
cm	=	centimeters
cm^3	=	cubic centimeters
COTS	=	commercial off-the-shelf
CO_2	=	carbon dioxide
FPGA	=	Field Programmable Gate Array
GRC	=	Glenn Research Center
JEM	=	Japanese Experiment Module (part of ISS)
JSC	=	Johnson Space Center
nm	=	nanometer
N_2	=	nitrogen
NH_3	=	ammonia
O_2	=	oxygen
OLGA	=	Optical Life Gas Analyzer
ppm	=	parts per million
psi	=	pounds per square inch
psia	=	pounds per square inch, absolute
RH	=	relative humidity
SBIR	=	Small Business Innovation Research
TEC	=	thermoelectric cooler
VCSEL	=	vertical cavity surface emitting laser
VDC	=	volts, direct current
VPI	=	Vista Photonics, Inc.
W	=	watts
WMS	=	wavelength modulation spectroscopy
WSTF	=	White Sands Test Facility

I. Introduction

There are a variety of both portable and fixed gas monitors onboard the International Space Station (ISS). Devices range from rack-mounted mass spectrometers to hand-held electrochemical sensors. An optical Multi-Gas Monitor has been developed as an ISS Technology Demonstration to evaluate long-term continuous measurement of four gases that are important from both life support and environmental health perspectives. Based on tunable diode laser spectroscopy, this technology offers unprecedented selectivity, concentration range, precision, and calibration stability.

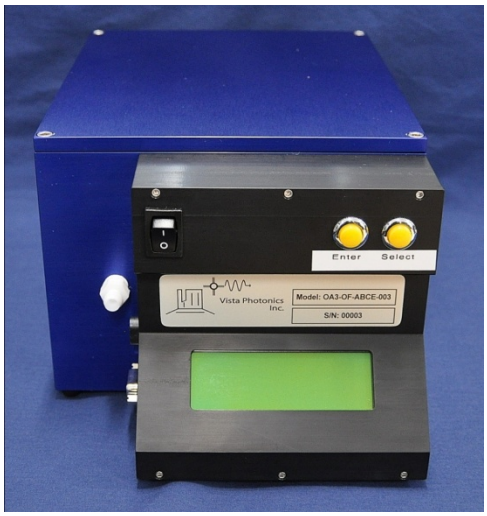

Figure 1. Version 2.0 Optical Life Gas Analyzer. *The vacuum tight enclosure met the requirements sought at the time of the development.*

The monitor utilizes the combination of high performance laser absorption spectroscopy with a rugged optical path length enhancement cell that is nearly impossible to misalign. The enhancement cell simultaneously serves as the measurement sampling cell for multiple laser channels operating within a common measurement volume. Four laser diode based detection channels allow quantitative determination of ISS cabin concentrations of water vapor (humidity), carbon dioxide, ammonia and oxygen. Each channel utilizes a separate vertical cavity surface emitting laser (VCSEL) at a different wavelength. In addition to measuring major air constituents in their relevant ranges, the multiple gas monitor provides real time quantitative gaseous ammonia measurements between 5 and 20,000 parts-per-million (ppm). A small ventilation fan draws air with no pumps or valves into the enclosure in which analysis occurs. Power draw is only about 3 W from USB sources when installed in NanoRacks or when connected to 28 VDC source from any EXPRESS rack interface. Internal battery power can run the sensor for over 20 hours during portable operation. The sensor is

controlled digitally with an FPGA/microcontroller architecture that stores data internally while displaying running average measurements on an LCD screen and interfacing with the rack or laptop via USB.

Figure 1 shows the first fully self-contained prototype version of the four gas optical sensor, constructed and delivered in 2011. That instrument was and is called the Optical Life Gas Analyzer (OLGA) version 2.0. Version 1.0 was a bread boarded open and exposed laboratory technology demonstrator. Because ammonia had been added to the required suite of sensed species, it was thought desirable to have the sensor in a hermetically sealed enclosure for prolonged exposure to that sticky molecule. In practice, it turned out easier to just put the whole sensor in a separate container for exposure to ammonia. The version 3.0 and 4.0 (Multi-Gas Monitor) devices are not isolated from the environment and employ in situ sampling with a DC fan.

Design, construction and certification of the Multi-Gas Monitor were a joint effort between Vista Photonics, Inc. (VPI) NanoRacks, LLC and NASA-Johnson Space Center (JSC). Vista Photonics developed the core technology and built the sensor. NanoRacks designed, constructed the aluminum enclosure, interfaces, and battery power management circuitry, integrated all subsystems into the enclosure, and then managed the certification tests, documentation and manifesting. The unit was calibrated in the JSC Environmental Chemistry Laboratory. The Multi-Gas Monitor was delivered onboard Soyuz as a technology demonstration to the ISS in November 2013 and activated in February 2014. The sensor is scheduled to operate for at least 6 months with data sent to the ground for evaluation. The primary goal is to demonstrate long term interference free operation in the real spacecraft environment.

The fundamental detection principle in each version of the sensor is path length enhanced optical absorption spectroscopy. Optical absorption spectroscopy provides signal that is linear and quantitative in concentration of the absorbing species for small absorbance. Wavelength modulation spectroscopy (WMS) allows measurement of weak optical absorbance by shifting the detection band to high frequencies, where laser excess ($1/f$) noise is reduced, to achieve fractional absorption sensitivities near the shot-noise limit (10^{-8}) in the laboratory. Field measurements using WMS routinely attain minimum detection absorbances of 0.001 % of the source light intensity under extended operation. WMS offers a sensitivity enhancement over direct optical absorption spectroscopy of a factor between 100 and 1000.

To implement WMS, a small amplitude modulation at frequency f is superimposed on the laser diode injection current, which causes modulation of the laser wavelength because wavelength is tuned by changing the current. The amplitude of the current modulation is chosen so that the induced wavelength modulation is comparable to the width of the spectral feature under study. Absorption by the target gas converts the laser wavelength modulation to an amplitude modulation that induces alternating current (AC) components in the detector photocurrent. Phase-sensitive electronics are then used to demodulate the detector photocurrent at a selected harmonic, nf (typically, $n = 2$) (Fig. 2). By implementing this technique at sufficiently high frequencies, $1/f$ laser noise is reduced and, occasionally, detector-limited sensitivity can be achieved.

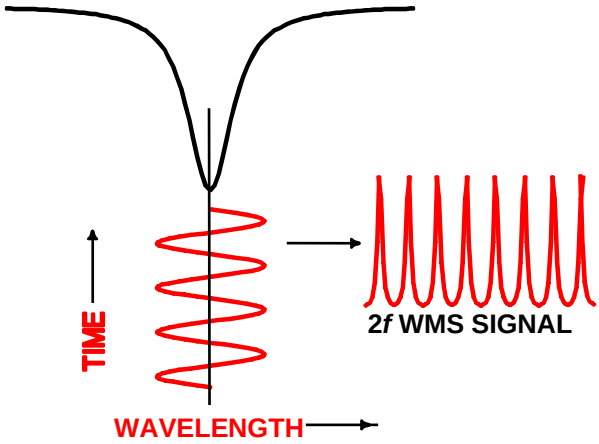

Figure 2. Generation of WMS signal. *Modulation of an optical source wavelength across the center of a molecular absorption feature produces WMS signal at twice the modulation frequency.*

In contrast, the Multi-Gas Monitor approach, which employs a special type of multi-pass cell, is limited to about 10^{-4} fractional absorbance by an effect called speckle interference. Speckle is caused by the granularity of the cell's diffusing material providing slightly different path lengths to the photodetector from each surface element. Speckle, while it is the limiting noise source, does not prevent detection of all the targeted gases at the required levels on spacecraft. The advantages of this cell relative to traditional multi-pass cells are in its compactness, ease of multiplexing and elimination of beam collection optics (which give rise to its rigidity/no alignment issues).

The near-infrared wavelength range is well suited for sensitive and selective detection of H_2O, CO_2, NH_3 and O_2 because many isolated suitable absorption features are available for each species. Careful selection of the nominal wavelength range can even result in several species being detected with a single laser device. Whereas current modulation and second harmonic detection provide the basic absorption signal at a single wavelength, simultaneous current or temperature tuning the laser wavelength at a lower rate can produce either a single isolated absorption

feature or an entire spectrum. In this case, the signal appears qualitatively as the second derivative of the original lineshape.

II. Optical Life Gas Analyzer

Many improvements had to be implemented to arrive at the final design of the version 4.0 flight-ready sensor prototypes. The 4.0 prototypes consist of the flight unit on ISS and the ground unit. The version 2.0 demonstrator device was extensively tested in 2011 and delivered in September, 2011. Many changes were implemented and tested in 2012 through the version 3.0 battery-operated prototype.

A significant challenge was to replace the COTS FPGA board used in the 2.0 sensor. Figure 3 shows that board on the right side in the photo. The board was bulky and ended up dictating the overall height of the sensor. It also included unnecessary and unused functionality while drawing excess power at too high a required input voltage. The board also required cumbersome ribbon cable connections to the microcontroller and main electronics board, which affected the width of the sensor enclosure. In contrast, the custom FPGA board on the left in Figure 3 is only a little larger than a business card. It provides direct connectivity to the microcontroller shown and is itself directly connected to the main electronics board, not shown. It also draws half the current of the COTS board (at 5 VDC) and provides only the needed functionality. The FPGA can be programmed *in situ*.

Figure 3. Custom and COTS FPGA. *Reduction of the electronics footprint was enabled by using the custom FPGA board in the left of the photograph.*

The version 3.0 sensor (Figure 4) introduced a great deal of autonomy into the platform that was absent in version 2.0. On power up, the sensor was allowed to start the lasers in a staggered timing sequence and begin measuring their respective species without any user intervention. The earlier sensor version required additional button depresses to get started. The software was further streamlined so that data was written to the onboard compact flash card every 2.5 s with simultaneous updates to the LCD. The LCD was upgraded to a physically larger, easier to read, one relative to the LCD in Figure 1 though the row and column counts are the same with no power cost. OLGA version 2.0 only updated the LCD and saved data about every 7 s. OLGA 3.0 also exclusively runs from camcorder batteries used on ISS. Two batteries power the sensor for about 36 hours with a third battery for running the 5 VDC fan. The sensor shuts down automatically once the voltage drops below a critical threshold. The batteries, operating in parallel, may be hot swapped. The newer version was also designed to utilize the onboard temperature and pressure measurements to convert water vapor concentration in ppm to relative humidity (RH) on a secondary screen.

Figure 4. OLGA version 3.0. *The custom FPGA board plugs directly into the main analog electronics board that controls the lasers. The sensor updates the significantly larger LCD and writes to file every 2.5 s, faster than the 7 s of earlier versions.*

OLGA 3.0 highlighted some deficiencies in the long term operation of

the architecture that needed to be addressed in the prototype flight unit. OLGA 4.0, renamed the Multi-Gas Monitor, implemented laser line locking of each VCSEL channel to eliminate wavelength drift in the sensor. This critical feature was lacking in version 3.0, which was designed and assembled in only two months to meet the delivery deadline. Because the lasers were free running, their wavelengths could drift around slightly and cause the sensor to misinterpret the absorption line of interest. This was made clear during a NASA press conference where OLGA 3.0 was displayed in operation. The sensor displayed an anomalous, high, reading for ammonia because a slight wavelength drift had caused it to interpret a water vapor line as ammonia. This potential issue had already been recognized and remedied in OLGA 4.0 at the time of the press conference, but the sensor had not yet been delivered.

The Multi-Gas Monitor scans farther in wavelength space than OLGA 3.0 for most of the sensor channels so that a sufficient spectral pattern can be obtained to unambiguously identify the line of interest for quantitative detection. The sensor continually updates the VCSEL operating temperatures to keep those target lines at the proper locations in the spectrum. This necessitated bidirectional communication between the FPGA and the microcontroller, which was implemented for the first time on the 4.0 platform.

Figure 5. Sensor version 4.0, Multi-Gas Monitor. *Flight prototype version 4.0 after assembly and integration. The adaptor plate allows for mounting to ISS equipment racks. The sensor can be powered through two USB ports or 28 VDC rack power.*

A second significant advancement over the 3.0 platform was the introduction of USB data transfer. During development of the basic architecture, it was not too burdensome to simply transfer data by physically removing the CompactFlash card and manually transferring data onto a computer. All versions up to OLGA 4.0 used this approach. Clearly ISS crew members cannot use this approach since they would need to open the sensor to access the card. Instead, a custom USB data board was designed and programmed to log the data internally to redundant, synchronized, microSD cards while appearing to the outside as a USB thumb drive. Consequently, data transfer is as simple as connecting a USB cable to the sensor's data port and transferring files by dragging and dropping in Windows.

The electronics architecture in the prototypes is comprised of one main electronics board, an FPGA board, a microcontroller, the USB communications and power boards. Design of the main analog board was continually improved throughout the development process of all the versions. The function of the main analog board is to provide current drive capability for the four laser channels and control their associated TECs without cross talk from the digital waveform delivered by the FPGA. The main board also routes power to the FPGA and microcontroller boards and two small photodetector preamplifiers. It also contains onboard temperature, pressure and humidity sensors. In versions 3.0 and earlier, sensor set-up was accomplished by determining the required laser operating parameters with the more flexible COTS FPGA device and then burning the specific program onto the smaller custom FPGA device. In version 4.0 the custom FPGA was configured so that the laser operating parameters could each be adjusted directly. This eliminates significant assembly/disassembly time.

Figure 6. Multi-Gas Monitor display. *Flight prototype instrument displays four measured gas concentrations, temperature and pressure. Display updates once per second.*

Portable power is provided by rechargeable batteries. A strict USB power only port and a combined power/data port provide power to the device when plugged in and also keep the batteries charged. The device can also be powered by 28 VDC EXPRESS rack power, so that it could be semi-permanently operated anywhere on ISS that such power is available. The various power sources can be connected and disconnected while the sensor is operating. Figure 5 shows the prototype flight unit with associated cabling and mounting plates and Figure 6

provides a close up of the active sensor display. The sensor front panel LCD presents measurement updates every second. A user will immediately see changes registered on the display in real time. However, due to the time limitations in exchanging the sample volume in the sensor with a DC fan operating below full capacity (for acoustic reasons) and the large amount of data acquired, it was decided to only write measurements to file once every 30 seconds. The sensor begins a new, dated and sequentially numbered, file at the start of each day in Coordinated Universal Time. The sequential numbering protects against loss of the correct date in the file naming system. Data is appended to the file as it is acquired onto a redundant, synchronized set of microSD cards inside the Multi-Gas Monitor. From the operations room at NanoRacks LLC, data files are selected and down linked as scheduled via the EXPRESS Rack ethernet and KU band transmitter. Downlinks are typically once a week.

A. Oxygen and Water Vapor Channels

Oxygen and water vapor are measured using VCSELs around 760 nm and 950 nm, respectively. Due to the short visible and near-infrared wavelengths both signals are obtained using simple inexpensive silicon photodetectors. The silicon photodetectors are not sensitive to the longer wavelengths employed for CO_2 and NH_3. Nonetheless, for ease of implementation, all four VCSEL channels are operated in a time division multiplexed mode so that the electronics cycle through each laser sequentially. Each channel is sampled at 2 Hz.

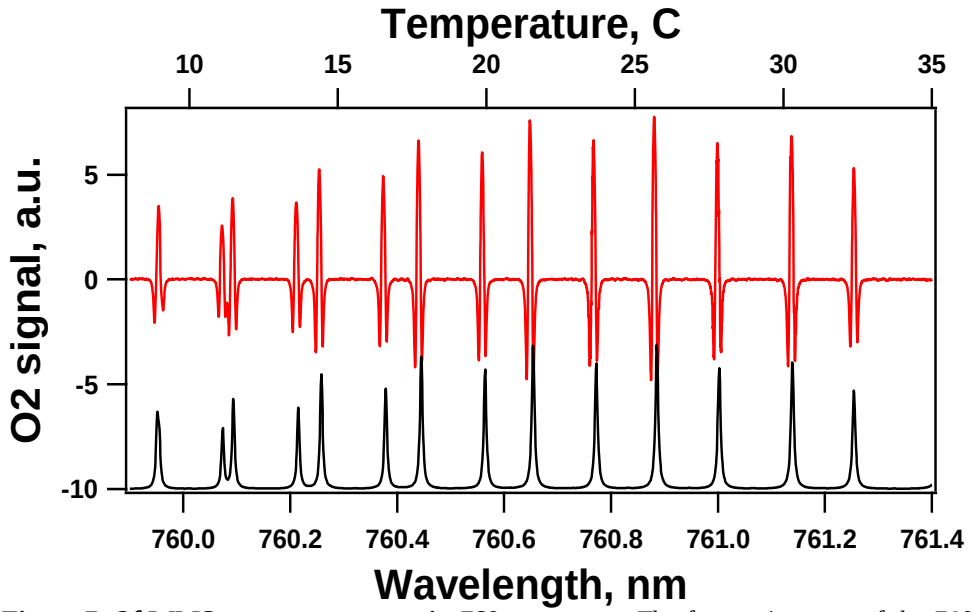

Figure 7. 2*f* WMS oxygen spectrum in 760 nm range. *The fast tuning rate of the 760 nm VCSELs allows access to many suitable absorption features for oxygen. The line at 760.68 nm is used on the OLGA prototypes. The red curve shows the 2f WMS data and the black shows a database spectrum.*

Oxygen: There are two regions on either side of 762 nm for oxygen detection accessible with COTS VCSEL devices. The early OLGA O_2 sensors used lasers operating on either side but version 4.0 operates around 760.6 nm. The advantage of this line is twofold. The line is the strongest in the entire spectrum, providing the highest sensor performance. More importantly, the density of lines is higher than on the other side of 762 nm and thus allows a smaller wavelength scan to establish a pattern for line locking. As with all the channels, WMS with second harmonic lock-in detection produces absorption spectra with qualitative second derivative lineshapes. Figure 7 shows the spectrum obtained for O_2 by tuning the VCSEL wavelength with temperature. Second derivative lineshapes are marked by a positive central peak with negative side lobes (troughs) on each side. When the depth of the wavelength modulation is optimum, the side lobe amplitudes are about 60 % of the amplitude of the peak. Raw signal is determined by measuring the peak-to-trough amplitude over the spectral feature. The black trace shows the spectrum simulated from the HITRAN database. Gross changes in wavelength are accomplished by controlling the laser temperature which is why the control electronics are capable of maintaining the set temperature to better than 0.01 C. The VCSEL devices tune much farther for a given change in temperature than distributed feedback laser diodes (30 GHz·°C^{-1} vs. 12 GHz·°C^{-1}). The tuning rate with current is likewise much faster than that of laser diodes. This

results in much less amplitude modulation associated with the desired wavelength modulation, making O_2 detection easier.

In addition to the higher frequency wavelength modulation, the nominal region of the selected line is scanned rapidly with a VCSEL current ramp which allows collection of at least two peaks in the spectrum. This allows determination of the exact spectral feature(s) under study through the pattern recognition algorithm from the microcontroller and consequent line locking capacity.

The fundamental detection capacity and precision performance of the OLGA versions has not changed much throughout their development. This is primarily because the fundamental performance is dictated by speckle in the optical path length enhancement cell, and that is not going to change. There were some improvements required along the way to allow the low-power FPGA/microcontroller architecture to achieve the performance of earlier microcomputer based prototypes. Of course, low frequency signal drift has been eliminated by the wavelength line locking. However, from a measurement precision standpoint, each sensor version is about as good as any other. Consequently, calibration and challenge plots that follow may have been obtained anywhere from versions 1.0 and 2.0 back in 2011 to 4.0 in 2014.

Figure 8 shows concentration challenge data obtained from the path length enhanced O_2 sensor channel after calibration in the Environmental Chemistry Laboratory at JSC in April 2011. There is clearly a significant time lag between the step challenges and the sensor response approaching the steady state. This is a consequence of the sensor being sequestered in a fairly large volume enclosure that required a long time for volume exchange. The inherent full response time of the sensor itself is set at 30 s by signal averaging according to predetermined requirements. The fastest possible response of any one of the four channels is 0.5 s. Glitches in the time trace data are due to the gas flow dilution blending system being reset.

Before pressure and temperature correction were added during system integration, the oxygen short term measurement precision over 12 hours is about 0.05 % at one standard deviation. Oxygen measurement accuracy is about 0.2 % at total concentrations between 5 % and 32 %.

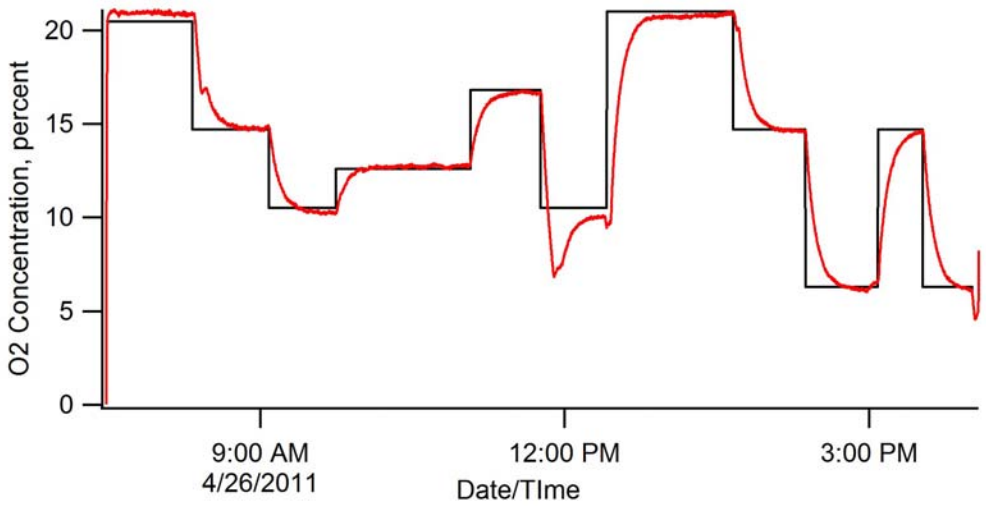

Figure 8. Oxygen concentration challenges at JSC. *An example of a time-series data set obtained by acquiring the OLGA oxygen signal over about 8 hours on 04/26/2011. Black trace: feed concentration; red trace: OLGA measured [O_2].*

Water Vapor: Water vapor measurement and calibration presents a special challenge due to its stickiness. There are also multiple ways of representing the water concentration including mole fraction (ppm) and relative humidity. The preferred representation depends on the specific user. The native measurement of the WMS technique is ppm. However, it is desired to have the sensor report water vapor levels in %RH. Vaisala, Inc. produces a water vapor sensor that provides sufficient precision to use as a transfer standard. The challenge with flow diluting water vapor from a temperature controlled cell is that it gets adsorbed on surfaces downstream of the blender. The Vaisala water vapor sensor was collocated in the same enclosure as the OLGA sensor and presented with challenge levels of humidity from the bubbler-based gas blending system. Figure 9 shows the targeted water vapor line at 948.5 nm in the spectrum on the left. The graph on the right shows OLGA measured signal plotted against the water vapor

concentration in ppm determined by the Vaisala. Some rollover in the ideal linear response is evident as the absorption signal enters the non-linear regime at high concentration. The non-linear least squares fitting algorithm is applied to the analytically correct functional form for the enhanced path length technique used in the cell. The data were obtained over the course of several days in conditions of both increasing and decreasing humidity. Hysteresis in wetting and drying is primarily responsible for the scatter around the best fit curve. Water vapor measurements in ppm are converted to RH by determining the partial pressure of water vapor from the mole fraction and total pressure and referencing that to the saturation vapor pressure of water vapor determined by the Antoine equation at the measured temperature. RH short term precision is about 0.05 % at one standard deviation and accuracy is about 1 % and could be improved with more extensive calibration or a better methodology.

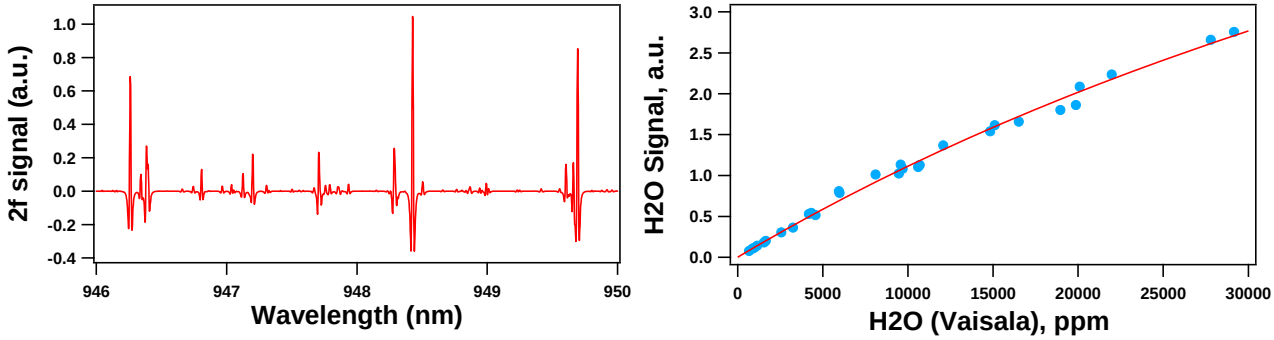

Figure 9. 2*f* WMS H_2O spectrum in 948 nm range and calibration. *The fast tuning rate of the 948 nm VCSELs allows access to many suitable absorption features for water vapor. The line at 948.4 nm is used on the OLGA platform. At high concentrations curvature is evident in the fit against concentration and reduces precision slightly at high relative humidity.*

B. Carbon Dioxide and Ammonia Channels

The second set of gas species are detected using more expensive InGaAs photodetectors since both VCSEL wavelengths are farther into the near-infrared at 2003 nm and 1512 nm for carbon dioxide and ammonia, respectively. These two channels are interleaved seamlessly with the previous two channels that use the silicon photodetector. A cycle of all four channels is accomplished twice per second. The utilization of various photodetectors does not impact the time division multiplexing approach and all channels could utilize a single common photodetector were one available that had responsivity across the full required wavelength range.

Carbon dioxide: Carbon dioxide has a strong absorption band in the 2000 nm range where VCSEL sources are available in a variety of configurations. There are also a few water vapor absorption lines scattered in this region, though they are weaker than the 948.5 nm line and offer lower sensitivity than this preferred wavelength. However, they are very useful in establishing the pattern for line locking since the carbon dioxide lines alone are quite regularly spaced. Figure 10 shows the WMS signal obtained in this wavelength range in humid ambient air. The regularly spaced lines across the spectrum belong to CO_2 and the two strongest lines in the spectrum belong to water vapor. They are larger, not because of high absorption strength, but because water vapor is present at about 20,000 ppm in the laboratory whereas carbon dioxide is present at about 400 ppm in ambient terrestrial air. The line at 2003 nm was selected because it has relatively high absorption strength, high selectivity in the presence of water vapor and is in a region where an unambiguous line locking pattern is available. The line locking pattern is obtained by rapidly current scanning the VCSEL wavelength between 2002.5 nm and 2003 nm. This has an additional advantage in that there is an isolated ammonia absorption feature in the range. While not as strong as the ammonia targeted VCSEL around 1512 nm, it is easily capable of corroborating the presence of ammonia at high levels. The Multi-Gas Monitor is configured to report ammonia from this channel once the level exceeds 1000 ppm. This region was also selected because the carbon dioxide measurement itself is not impacted significantly by the presence of large concentrations of ammonia.

Calibration of the Multi-Gas Monitor required about a week at JSC in July 2013 and spanned a wide range of concentration challenges for all four sensed species. In order to get as many calibration points as possible for each gas, the flow dilution of the carbon dioxide certified standards was done in such a way that the oxygen concentration was also highly controlled but variable. The graph on the left of Figure 11 shows the sensor step response to oxygen and carbon dioxide over the course of a day during calibration. Each of these points was precisely determined by the

gas blending system. Simultaneous calibration of carbon dioxide and oxygen was facilitated by their not being sticky and proceeded rapidly. Any irregularities in the time trace are due to the switching of the certified gas standards. The graph on the right of Figure 11 shows the calibration curve of the sensor response against the set carbon dioxide concentration. Some non-linearity at the higher concentrations is evident and due to the high absorbance at those levels. As with water vapor, the data are fit to the correct analytic form for the high absorbance and the nature of the enhanced path length approach employed. The carbon dioxide short term measurement precision is about 20 ppm and accuracy ranges from 60 ppm at low concentrations to 5 % of the reading at the highest concentrations. At typical spacecraft concentrations (3000-5000 ppm), carbon dioxide can be resolved into several hundred parts.

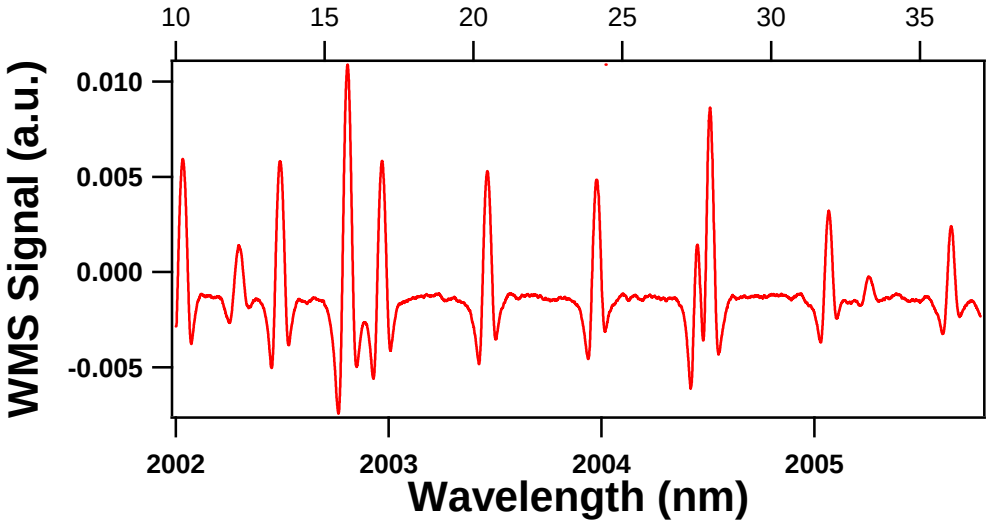

Figure 10. Carbon dioxide and water vapor absorption spectrum in the 2003 nm wavelength range. *The largest lines are due to water vapor at high background concentration. Carbon dioxide is targeted at 2003 nm, where it is immune to cross sensitivity from water vapor. The line is strong, isolated, and able to provide reliable CO_2 determination at spacecraft relevant levels.*

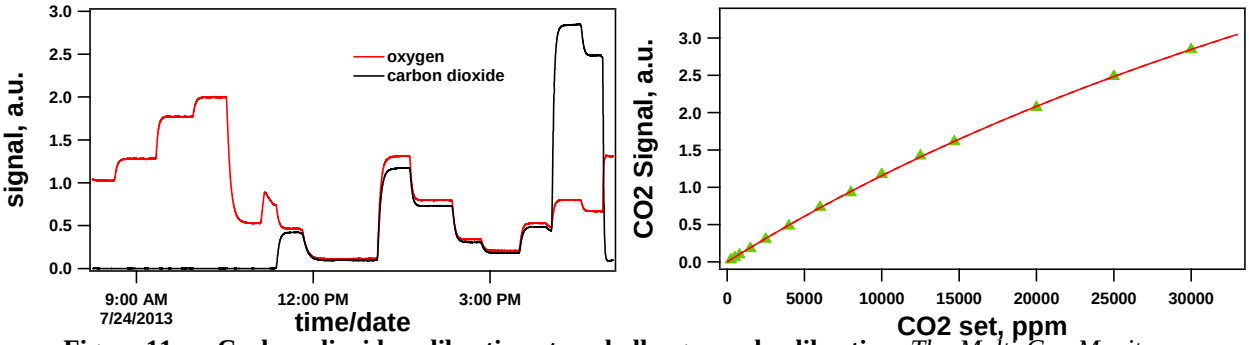

Figure 11. Carbon dioxide calibration step challenges and calibration. *The Multi-Gas Monitor was simultaneously calibrated with step challenges of oxygen and carbon dioxide. At high concentrations curvature is evident in the fit against concentration but is easily accommodated by the fitting algorithm.*

Ammonia: Two OLGA ammonia sensors — OLGA 2.0 A and OLGA 2.0 B — operating with VCSELs at 1512 nm were calibrated and extensively tested simultaneously at NASA WSTF in August 2011. Both sensors were tested using the same sample gas flow. The sensors were placed in a plastic bag, which had feed through orifices for the inlet and outlet gas lines and electric wires (power supply and serial interface cables). For both sensors, the lids were removed to ensure fast circulation and mixing of the sample gas inside the sensor enclosure box. The OLGA 2.0 A sensor was placed closer to the gas inlet; the OLGA 2.0 B was placed closer to the gas outlet. The sample gas was supplied to the test volume at a rate of 5–9 liters per minute. The graph on the left of Figure 12 presents the

time-series data sets acquired by the OLGA 2.0 A sensor and the one on the right for the OLGA 2.0 B sensor. The series was started by presenting a 4980 ppm NH_3 mixture to "passivate" the surfaces of the system with ammonia to improve the time response. After about half an hour, the air flow was reconfigured to bypass the humidifier to reduce the gas humidity. It was expected that low humidity could result in faster response. In practice, only a slight improvement in the system response to changing the ammonia concentration under dry conditions was observed. On the other hand, switching from moist 4980 ppm NH_3 to dry 4980 ppm NH_3 did not show any significant changes in the OLGA signal amplitude. Independence of the ammonia signal from relative humidity was assumed in subsequent experiments and dry gas samples were used. A small bump at about 11:00 am in both sensors time traces corresponds to the start of the flow program, which required resetting of the flow control system. The flow program locked up at about 1:50 pm; after that time the concentrations were set manually. Both sensors showed nearly equivalent response and precision. Any difference in raw signal is due to different photodetector amplifier gain settings.

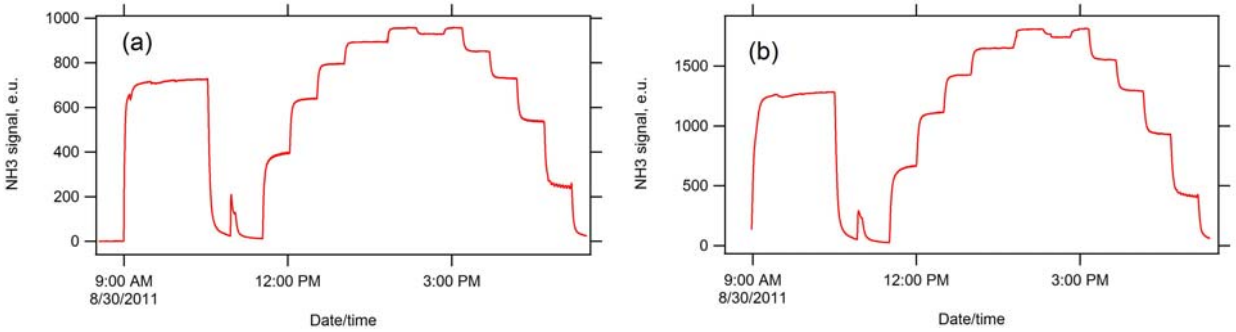

Figure 12. Ammonia calibration step challenges. *The first high concentration calibration for ammonia at 1512 nm was done at NASA WSTF in August 2011. Two redundant OLGA 2.0 sensors were simultaneously calibrated from 1,000 ppm to 10,000 ppm. Both sensors displayed about equal performance after accounting for time lag of the sensor farther down stream.*

A preliminary, cursory, calibration of both sensors had taken place the day before the data of Figure 12 were acquired. That was necessary as the testing and gas blending methodology needed to be established in real time before the actual calibration the following day. The graph on the left in Figure 13 shows both the preliminary and main calibration plots for the OLGA 2.0 A sensor using the correct analytic form for the signal dependence first implemented at that time. For both independent sensors, the main calibration is very similar to the preliminary one. The differences at lower NH_3 are caused by the differences in the total flow (7,000 cc/min for main calibration versus 9,000 cc/min for preliminary calibration). After final calibration, both OLGA sensors were challenged with gas samples containing ammonia concentrations known only to the NASA test conductor. The set ammonia concentrations were disclosed to Vista Photonics personnel only when the testing was over. The graph on the right

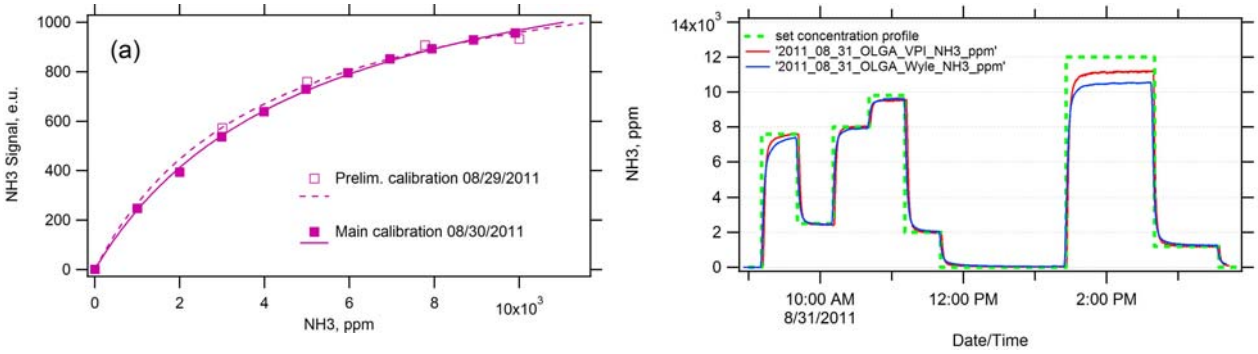

Figure 13. Ammonia calibration curves and blind step challenges. *Both a preliminary and full calibration for ammonia show good agreement though obtained on different days. Curvature from high absorbance is accounted for in the fitting algorithm. Blind step challenges done after the full calibration show good agreement of both OLGA sensors with the blind set concentrations. Low readings at the highest 12,000 ppm set point were due to the lower flow rate available at that concentration.*

of Figure 13 shows the time series data of the testing for both OLGA sensors (red trace: OLGA 2.0 A; blue trace: OLGA 2.0 B). The set concentration profile is shown with dashed green lines. Generally, both sensors demonstrated very good performance over the whole required range of ammonia concentrations (1000–10,000 ppm). One

challenge concentration was set at 12,000 ppm, which was outside of the calibrated range at that time. Both sensors underestimated this concentration, however note that to generate 12,000 ppm the flow system had to be operated at a very low 5,000 cc/min total flow, which could result in lower actual concentration being presented to the sensors. This is corroborated by the sensor that was farther downstream underestimating the concentration more than the one closer to the flow, indicating surface passivation effects are to blame. During calibration of the Multi-Gas Monitor in July 2013 at JSC, ammonia concentrations up to 20,000 ppm were presented and they followed the basic behavior of the Figure 13 calibration curves. Ammonia short term measurement precision is about 2 ppm and accuracy is about 6 ppm at low concentrations and a few percent of the reading at the highest concentrations.

C. Atmospheric corrections

Each gas channel is calibrated under carefully controlled conditions of temperature and pressure. The nominal calibration is referenced to 298 K and 760 Torr. Onboard pressure and temperature sensors are then used to correct the measured concentrations when those parameters deviate from the reference values. The corrections are typically determined empirically when that is feasible. In most cases linear temperature corrections turn out to be sufficient since the span of temperature is relatively small (285 K to 305 K). Quadratic terms are included in the pressure corrections because of the larger span (500 Torr to 800 Torr). An onboard electronic RH sensor could be used to correct the concentration determinations but the effect of RH on the absorption linewidths is too small to warrant the effort. Instead, the electronic RH determination is used as a self consistency check against the optical water vapor determination.

III. Multi-Gas Monitor on the International Space Station

Following calibration and assembly of the version 4.0 prototype flight sensor, now called the Multi-Gas Monitor by NASA, the sensor was put through various tests under the guidance of NanoRacks LLC who specialize in getting unique payloads to ISS. These included vibration, electromagnetic interference, acoustics and off-gas testing. NanoRacks owns the rack where the sensor resides on ISS and is responsible for data transfer to the ground and data distribution to stakeholders. The sensor was also put through several final gas challenge points at JSC immediately prior to shipment to the Soyuz launch site at Baikonur, Kazakhstan.

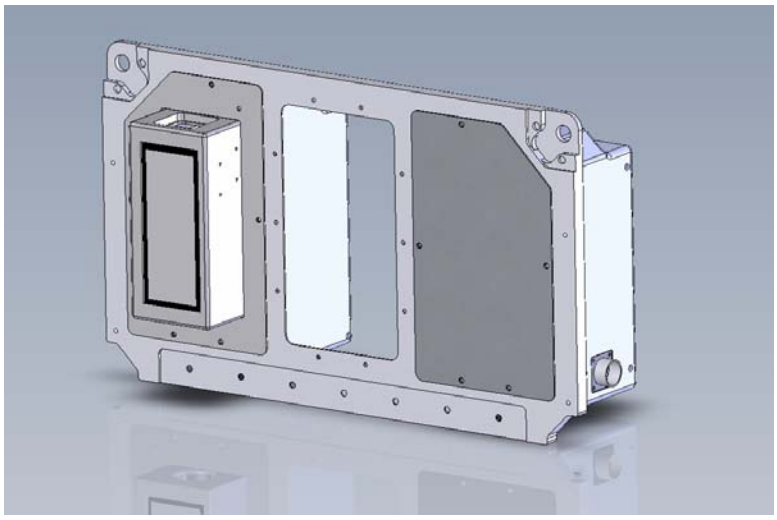

Figure 14. Drawing of Multi-Gas Monitor in ISS locker. *The sensor is mounted onto the front of the locker so that it can draw in a local sample with a fan and exhaust it back into the environment. Many other experiments may be operating in the locker.*

The sensor was launched to the ISS on November 7, 2013 aboard Soyuz TMA-11M and remained stowed on ISS until early February 2014. On February 3, 2014 the Multi-Gas Monitor was installed and activated in the NanoRacks Frame 2 locker, Figure 14, in an EXPRESS rack in the Japanese Experiment Module (JEM). As part of the activation and check out (ACO), a crew member conducted a quick test to verify sensor functionality by breathing directly into the monitor's intake. The sensor properly registered a rapid increase in carbon dioxide and water vapor and their subsequent decay. The peak CO_2 value was called down, and the video of the ACO showed a maximum reading of 5015 ppm.

Figure 15 shows the Multi-Gas Monitor during operation aboard ISS on February 10, 2014 (upper right part of the photograph, arrow). The locker is upside down relative to the Figure 14 drawing. In the photo flight engineer Michael Hopkins is preparing an experiment with two devices called SPHERES-RINGS in the foreground. It is worth noting that the experiment is within a few feet of the Multi-Gas Monitor and that the sensor is directly sampling the air in front of it. In addition to the normal data stream that just includes the four species measured concentrations, measured ambient conditions, and esoteric internal sensor information, another file is written at the end of each day that is comprised of the raw spectrum from the four VCSEL channels at that moment in time. This

file allows investigators on the ground to apply their own spectral pattern recognition experience to verify that the sensor line locking is never confused. As an example, the raw spectrum from aboard ISS on February 11, 2014 is presented in Figure 16. In the Figure each gas sensing channel is assigned to its own quadrant and there are 256 spectral bins for each gas or VCSEL. The spectral file also contains information about where the line locking index for each channel is relative to the allowed bounds. In each case in Figure 16 there is actual gas corresponding to that measured species in each channel except for ammonia, which is not typically expected to be present on ISS within the few-ppm detection limit of the sensor. The two small absorption features in the ammonia channel are due to water vapor and are used for line locking the ammonia VCSEL. That way the sensor will always be looking in the right place to detect an ammonia contingency should one occur. If the detected ammonia concentration ever exceeds 100 ppm, the sensor will begin interleaving saved spectral files every 30 seconds with the regular data until the concentration drops below the 100 ppm threshold. This allows investigators on the ground to unambiguously identify an ammonia contingency as this could inform the decision process of ISS managers. An ammonia challenge to the sensor is scheduled to be conducted during the 6-month technology demonstration period.

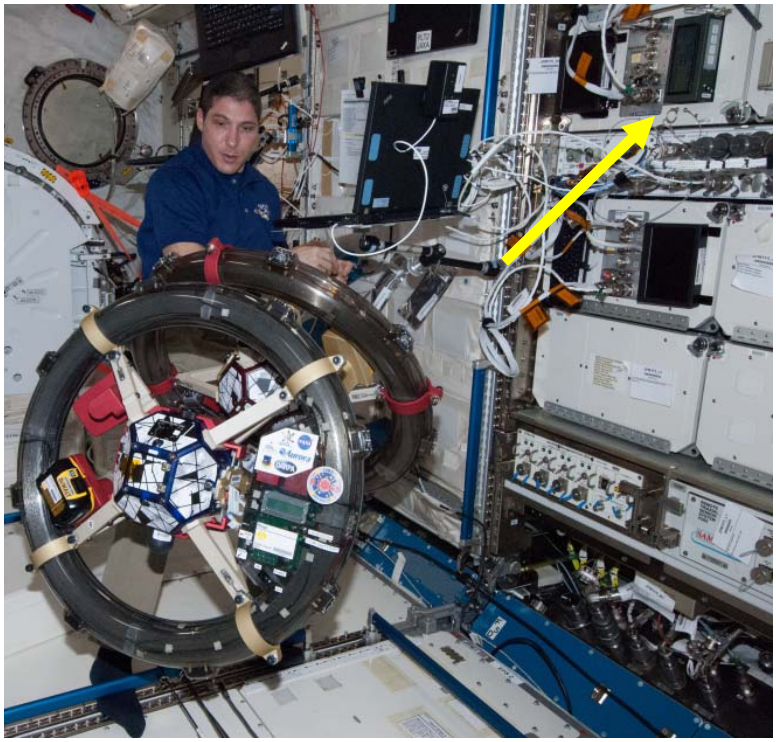

Figure 15. Multi-Gas Monitor operating in the JEM on ISS with SPHERES-RINGS nearby. *NASA photo ISS038E045621*

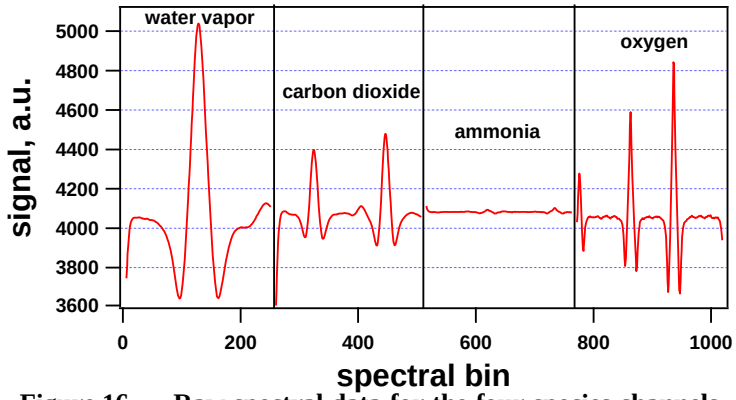

Figure 16. Raw spectral data for the four species channels. *A spectrum for the four gases is saved once a day to provide visual verification that all lasers are operating properly.*

For example , Multi-Gas Monitor data are shown beginning from activation until February 12, 2014 in Figure 17. The data are consistent with other data obtained on ISS from non-portable devices. Clear daily cycles in carbon dioxide and humidity are evident and well-established on ISS. Oxygen is slightly elevated relative to Earth-ambient, but consistent with other sensors. Noise on the ammonia channel is typically below 5 ppm, the lowest value allowed to report to the LCD (results below that display as < 5 ppm). Actual measured values are contained in the data file except that any negative values are reported as zero for all species. RH determination is dependent on the temperature at the location of the measurement and the temperature inside the sensor is consistently about 5 °C above the ambient JEM temperature while inside the locker. Consequently, RH measurements presented in Figure 17 are corrected using this differential. The LCD values reported in real time on the actual sensor are about 10 % RH lower than those in the Figure. In the future, a separate ambient temperature measurement (at the air intake) will be included for correcting the RH determination. The sensor's fundamental determination of water vapor mole fraction in ppm is not affected by this temperature differential. There are two seemingly anomalous spike events on the carbon dioxide time trace in Figure 17. Unlike the initial breath test, the spikes are not accompanied by a concomitant increase in water vapor. The culprit in the second event is revealed by Figure 15 and the SPHERES-

RINGS experiment. SPHERES is able to station keep and maneuver within ISS using compressed CO_2 gas thrusters. Careful examination of the carbon dioxide time trace during a spike event reveals individual thruster firings, Figure 18. SPHERES was also active on JEM during the event on February 7, 2014. Although unexpected, these carbon dioxide sensor challenge events demonstrate the utility of having real time monitors like the Multi-Gas Monitor distributed throughout ISS and, hopefully, future spacecraft, landers and habitats used for exploration beyond near Earth orbit.

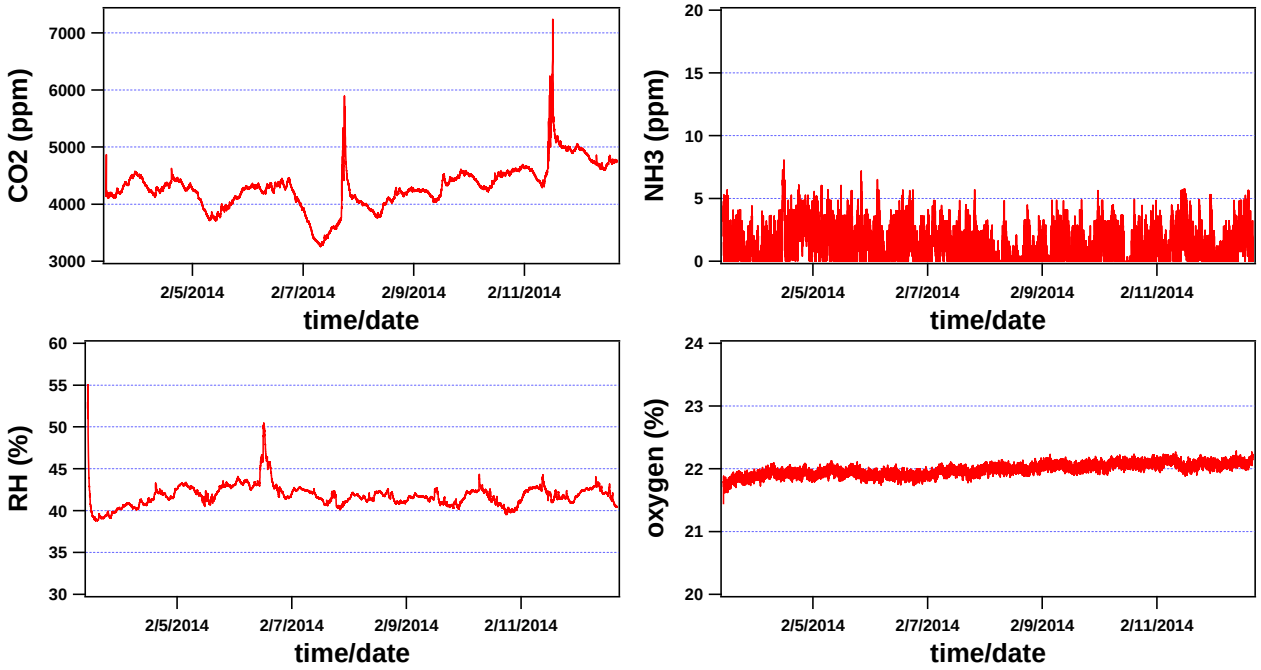

Figure 17. Multi-Gas Monitor concentration data obtained during the first week on ISS.

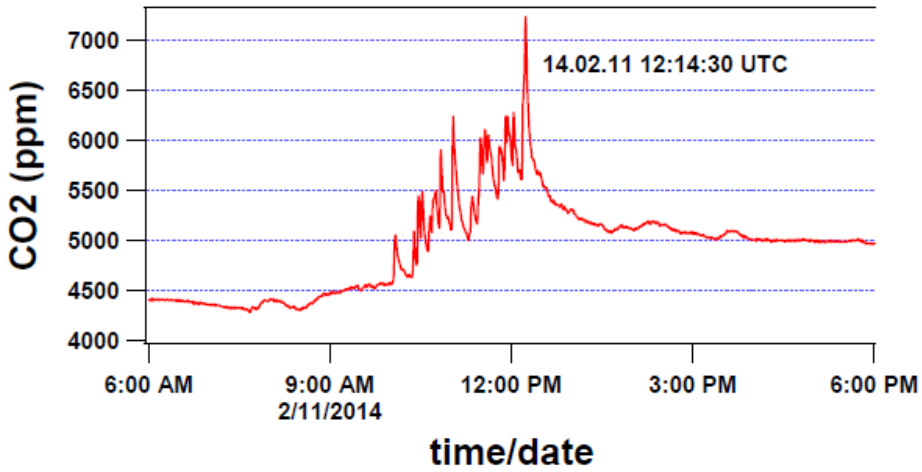

Figure 18. Close up of CO_2 behavior during event. *Carbon dioxide measurements by the Multi-Gas Monitor showed multiple spikes presumably from SPHERES-RINGS thrusters. After the event, the baseline carbon dioxide concentration was about 500 ppm higher.*

IV. Conclusion

An integrated optical and electronics architecture for multiple gaseous species detection has been developed

over several years through the Small Business Innovation Research program. Sensitivity and selectivity have been demonstrated and verified on the ground during multiple rounds of testing at JSC and WSTF. The platform presents a rugged, compact, low power sensor design suitable for portable measurement of critical species onboard spacecraft. A prototype device is operating on ISS after activation in February 2014. The OLGA/Multi-Gas Monitor architecture is also designed to be highly scaleable. In the future, a combustion product monitor variant within the same nominal enclosure volume could be added. Vista Photonics has participated extensively in combustion testing at WSTF and GRC for several years to develop this capability. A paper describing recent progress is a part of this conference.

Acknowledgements

The authors gratefully acknowledge the ISS Vehicle Office at JSC for funding the technology demonstration under NASA contracts NNJ13HB90C and NNJ13GA08C, Billy Wallace and Steve Beck of Wyle Laboratories for sensor calibration and off-gas testing, Jimmy Wines, Patrick Sinnot, Craig Walton, and Susan Lufkin for the expert electronics, mechanical, operations and documentation efforts at NanoRacks, and Steve Bress of Entropy Engineering for designing and programming the RS-232 to USB data interface/storage board.

Reference Section to be added later.